

Th P9 02

Visualization of Ultra-Weak Diffractors based on Vector Pair RTM

G. Erokhin* (IKBFU), A. Danilin (IKBFU), M. Kozlov (IKBFU)

Summary

The important problem for RTM-like methods is detecting diffractors on the background of the strong reflections. Conventional RTM images have original artefacts because the method RTM is based on the wave-equation. For overcoming such interference the regularization is performed by filtration in some extended space of seismic parameters. Method VPRTM in detail analyses the amplitudes and phases of two interconnected vectors: the particle velocity vector of the incident wave and the generated vector of the reflected or scattered wave. The new subsurface images, obtained by VPRTM method are more informative and precise than the conventional RTM images. The proposed approach demonstrates the high accuracy at the detecting weak diffractors on the background of strong reflections. Method VPRTM is perspective for the carrying out the precision analysis in the AVO, Dip, Frequency, Impedance, Reflectivity and Diffractivity procedures simultaneously.

Introduction

Imaging Condition is the key point for RTM image processing (Baysal et.al.,1983; Whitmore, 1983; McMechan, 1983). Conventional RTM images has original artefacts because the method is based on the wave-equation. For overcoming such interference the image regularization is performed by filtration in an extended space of parameters (Yoon and Marfurt, 2006; Sava and Fomel, 2006; Zhang and McMechan, 2011). Erokhin et. al., 2017, suggested the new approach for regularization, based on using the Interconnected Vector Pair Imaging Condition (IVP IC). The method, based on such approach is called Vector Pair Reverse Time Migration (VPRTM). In this paper we present the results of further developing the VPRTM method particularly at the example of detection the ultra-weak diffractors on the background of strong reflections for the model of West Siberia tight oil deposit.

Method

The mathematical statement VPRTM derives acoustical wave by the couple (p, \vec{u}) where p is the pressure and \vec{u} is the particle velocity vector field, which satisfy the first order linear differential equations (Erokhin et. al., 2017). The forward wave $(p^f, \vec{u}^f)(x, t; x_s), t \in [0, T]$ satisfies the Cauchy problem

$$\begin{aligned} p^f_t - c^2 \operatorname{div}(\nabla \vec{u}^f) &= r(t) \delta(x - x_s) \\ \vec{u}^f_t &= \nabla p^f \\ p^f|_{t=0} &= 0, \quad \vec{u}^f|_{t=0} = 0. \end{aligned} \quad (1)$$

Here $r(t) \delta(x - x_s)$ is the source located at the boundary point $x_s \in \Gamma = \{x \in \mathbb{R}^n | x^n = 0, n = 2, 3\}$ (δ is the Dirac function, and r is some wavelet), T is the time of observation. Let $p_0 = p^f|_{\Gamma \times [0, T]}$ be the “measured” pressure. The adjoint problem to the problem (1) is written as follows

$$\begin{aligned} p^b_t - c^2 \operatorname{div}(\nabla \vec{u}^b) &= 0 \\ \vec{u}^b_t &= \nabla p^b + p_0 \delta(x^n) \vec{\nu}_\Gamma \\ p^b|_{t=T} &= 0, \quad \vec{u}^b|_{t=T} = 0, \end{aligned} \quad (2)$$

where $\nu_\Gamma = (0, \dots, 0, 1)$ is the unit normal vector to Γ . We call (p^b, \vec{u}^b) the back wave since it propagates in reversal time. So, forward and back waves include two vector fields: $\vec{u}^f(x, t; x_s)$ and $\vec{u}^b(x, t; x_s)$. In what follows we use these vector fields only. Further we will use short notations $f = \vec{u}^f$, $b = \vec{u}^b$.

Thus, at each point in the space of the acoustic medium, we have a pair of interconnected vectors (b, f) that are characterized by their own amplitudes, phases, frequencies that vary with time and depend on the coordinates of the sources. Behavior of the backscattering vector at each point of the acoustic space depends only on the properties of the medium in the neighborhood of this point. Then the incident signal at the point of space can be considered as an input to a certain black box (medium), and the output is a backscatter signal. Each test signal at the input of such a black box will be called an event. It is obvious that the number of such events for each point of the medium is determined by the time sampling, the number of sources, and can reach several tens of thousands. In this case, each event for a two-dimensional acoustic medium has its coordinates in a six-dimensional space: time, source number, amplitude f , amplitude b , phase of incident angle α , phase of scattering angle β . For a three-dimensional acoustic medium, similar events will have two dimensions greater due to additional two spatial angles. Thus, events for the three-dimensional acoustic medium will be localized already in the eight-dimensional space. For the case of a three-dimensional elastic medium, events are localized in 12-dimensional space.

Let us $p = (p_1, \dots, p_6) = (t, s, |f|, \|b\|, \gamma, \theta)$ is a vector from compact set $P \subset R^6$, where $\gamma = (\alpha - \beta) / 2$ is opening angle and $\theta = (\alpha + \beta) / 2$ is the dip angle. Condition IVP IC (Erokhin et. al., 2017) is proposed based on admissible vectors pair. The procedure of the imaging media consists of the two stages. At the first stage we obtain admissible subset $Q_p \subseteq Q$. Subset is the result of filtration (regularization) the full set Q by not only restrictions of set $\{t_k, x_s | k=0, \dots, N_T, s=1, \dots, N_s\}$, but also by restriction of remaining components of vector $p = (t, s, |f|, \|b\|, \gamma, \theta)$ which belongs to subset $Q_p \subseteq Q$. For example such subset is $Q_p = \{t_k, x_s | k=0, \dots, N_T, s=1, \dots, N_s, \langle b, f \rangle / \|b\| \|f\| \leq c \leq 1\}$, where \langle, \rangle means scalar product and c some constant (similarly to approach Stolk et.al., 2009, Whitmore and Crawley, 2012). The design of admissible subset Q_p with angle-domain (α, β) or (θ, γ) restrictions is similar to filtration on the basis of local image matrix (Xie and Wu, 2002; Yan and Xie, 2009). At the second stage we choose the concrete type of IVP Imaging Condition, which is written as follows

$$I(x) = R_{Q_p}(f, b)(x), \quad (3)$$

where R_{Q_p} is some operator being applied to the pair of vectors (f, b) from subset Q_p . Such operator may be scalar product, product of modules of two vectors, division etc., with subsequent summation or calculation of averages or variances (Erokhin et. al., 2017). For example: $R_{Q_p} = R_Q(|b \| f|) = \sum_Q (|b \| f|)$ is exactly conventional RTM.

Examples

The important problem for RTM-like methods is detecting diffractors on the background of the strong reflections (Landa et al., 1987; Khaidukov et.al., 2004, Erokhin et.al., 2012). This problem can successfully be solved on the basis of the proposed VPRM approach (1)-(3), using a target filtration of vector subject to amplitude and phase features of distributions for reflection and diffraction points. Typical model for West Siberia tight-oil deposit is presented at Fig.1a. Six circular inclusions with diameters 20 meters (numbering of inclusions from left to right from 1 to 6) are introduced in the tight oil layer. Depth of tight oil layer is 2600 m. Background velocity in the tight oil layer is 3453 m/s. Inclusions velocities are from 3000 m/s up to 3500 m/s (from left to right). Distance between inclusions is 5000 m. Between and under inclusions #2 and #3 there exists natural fault. Computational parameters are: the spacing step is 10 m; the time step is 0.4 ms; the number of sources is 354; the source step is 50 m; the computational domain for one source is 4800x3200 m; the number of receivers is 97; the receiver interval is 50 m; dominant frequency of Ricker's wavelet is 40Hz. Simulated seismic data for this benchmark model are free shared (www.4dprm.com). Fig. 1b demonstrates the result of convetional PSTM processing. Tight oil layer is the second layer from below.

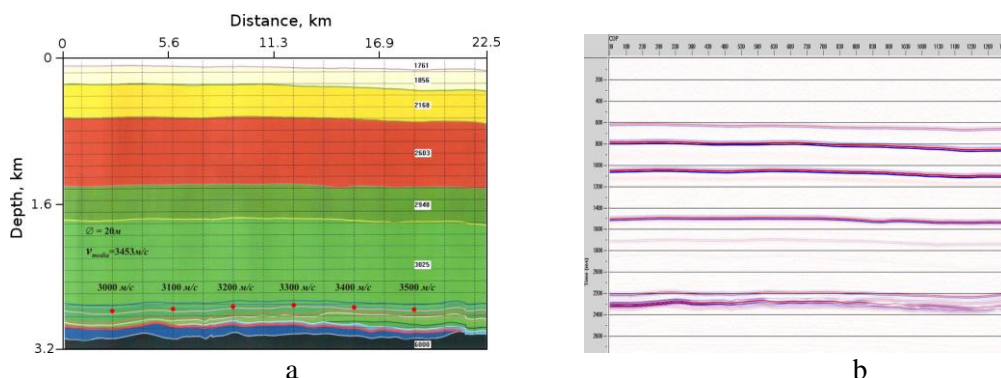


Figure 1 Typical model for West Siberia tight oil deposit with introduced six circular inclusions (a) and result of convetional PSTM processing (b)

The next Fig.2 shows the results of special processing for detecting diffractors by two methods. First method is called CSP (Erokhin at.al.,2012) and use the multidimensional spectral filtration (Fig. 2a). Second method is called Diffraction Imaging and use the full-azimuth subsurface angle-domain

decomposition based on the beam approach (Koren Z. and Ravve I., 2011) – Fig.2b. Result of Diffraction VPRTM processing is presented at Fig. 3. Here the IVP IC is $R_{Q_p} = R_{Q_p}(|b|) = \sum_{Q_p} (|b|)$, where admissible subset $Q_p \subseteq Q$ includes the events with the properties of mostly scattered waves. Result of VPRTM processing for estimation dip values near the inclusions is depicted at Fig. 4. For this case IVP IC is $R_{Q_p} = R_{Q_p}(|b|, \psi)$ and type of R_{Q_p} is statistical momets. Results of AVO VPRTM are presented at Fig.5: Poisson coefficient 6a and Fluid Factor 6b. Here the IVP IC is $R_{Q_p} = R_{Q_p}(|b|/|f|, \chi)$.

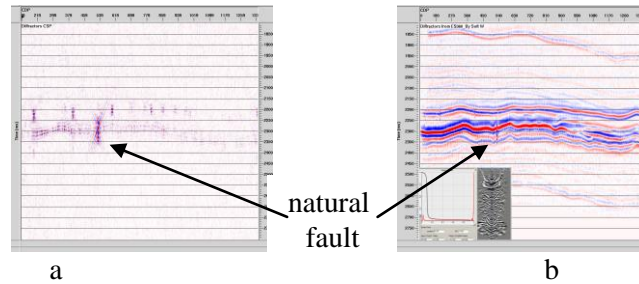


Figure 2 Results of special processing by CSP method (a) by Diffractivity Imaging method (b)

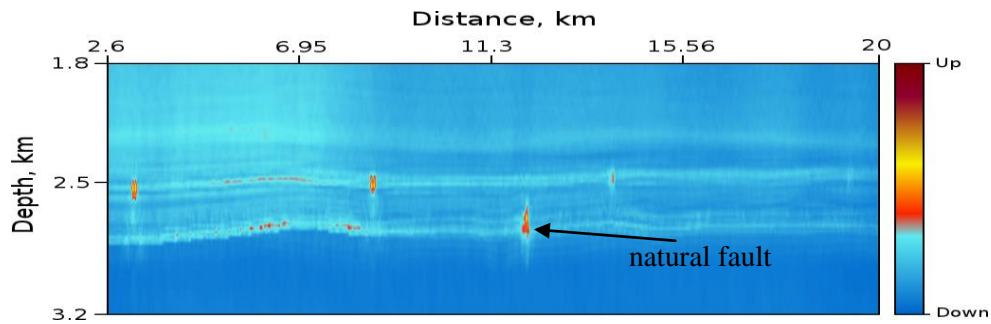


Figure 3 Result of Diffraction VPRTM processing with filtration non-scattered waves

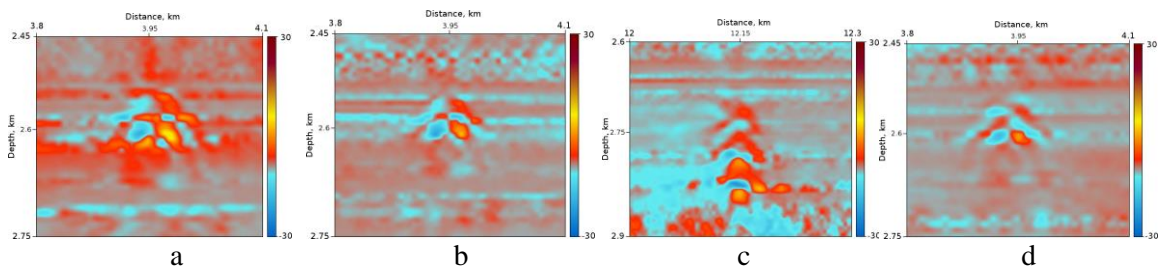


Figure 4 Result of VPRTM processing for estimation dip values near the inclusions #1(a), inclusion #2(b), natural fault (c) inclusion #3(d).

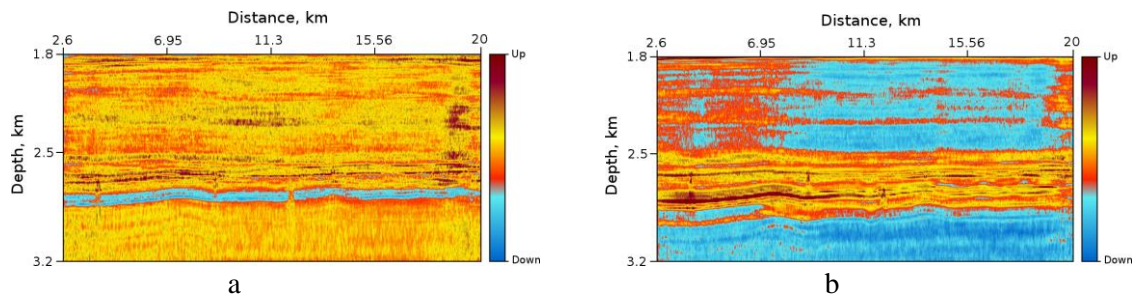


Figure 5 Result of AVO VPRTM processing. Poisson coefficient (a) and Fluid Factor (b)

Conclusions

The filtration procedures of interconnected vectors pair based on the Interconnected Vector Pair Image Condition are proposed. The subsurface images, obtained by VPRTM method are more informative than the conventional RTM images. New method has demonstrated the high accuracy at the detecting weak diffractors on the background of strong reflections. Method VPRTM is perspective for the carrying out the precision analysis in the AVO, Dip, Frequency, Impedance, Reflectivity and Diffractivity procedures simultaneously.

Acknowledgements

The authors thank M.Zvereva and S.Sergeeva for useful participation. This work is supported by the Russian Science Foundation under grant 16-11-10027.

References

- Baysal, E., D. D. Kosloff, and J. W. C. Sherwood, 1983, Reverse time migration: *Geophysics*, 48, 1514–1524, doi: 10.1190/1.1441434.
- Landa, E., Shtivelman, V. and Gelchinsky, B., 1987, A method for detection of diffracted waves on common-offset sections. *Geophysical Prospecting*, 35, 359-374.
- Koren Z., Ravve I, 2011, Full-azimuth subsurface angle domain wavefield decomposition and imaging Part 1: Directional and reflection image gathers; *Geophysics*, 76, S1-S13.
- Khaidukov V., Landa E. and Moser T.J. ,2004, Diffraction imaging by focusing-defocusing: an outlook on seismic super resolution. *Geophysics*, 69, 1478-1490.
- Erokhin, G.N., A.N. Kremlev, L.E Starikov, V.V. Maltcev, and S.E. Zdolnik, 2012, CSP-Method Prospecting of Fracture-cavernous Reservoirs in the Bazhen Formation of the Salym Oilfield: 74th Conference & Exhibition, EAGE, Extended abstract, Y028.
- Erokhin G., Pestov L.,Danilin A., Kozlov M., and Ponomarenko D., 2017, Interconnected vector pairs image conditions: New possibilities for visualization of acoustical media, 2017, SEG Technical Program Expanded Abstracts 2017: 4624-4629., <https://doi.org/10.1190/segam2017-17587902.1>
- McMechan, G. A., 1983, Migration by extrapolation of time-dependent boundary values: *Geophysical Prospecting*, 31, 413–420, doi: 10.1111/j.1365-2478.1983.tb01060.x.
- Sava, Paul, and Sergey Fomel, 2006, Time-shift imaging condition in seismic migration: *Geophysics*, 71, no. 6, S209–S217.
- Stolk, C. C., M. V. de Hoop, and T. Op't Root, 2009, Linearized inverse scattering based on seismic reverse-time migration: Proceedings of the Project Review, Geo-Mathematical Imaging Group (Purdue University, West Lafayette IN), 91–108.
- Whitmore, N. D., 1983, Iterative depth migration by backward time propagation:53th Annual International Meeting, SEG, Extended Abstracts,382–385.
- Whitmore N. D., and Sean Crawley, 2012, Applications of RTM inverse scattering imaging conditions: 82nd Annual International Meeting, SEG, Expanded Abstracts, doi: <http://dx.doi.org/10.1190/segam2012-0779.1>
- Xie, X., and R. S. Wu, 2002, Extracting angle domain information from migrated wavefields: 72nd Annual International Meeting, SEG, Expanded Abstracts, 1360–1363.
- Yan, R., and Xie, X.-B., 2009, A new angle-domain condition for prestack reverse-time migration: 79nd Annual International Meeting, SEG, Expanded Abstracts, 2784-2788
- Yoon, K., and K. J. Marfurt, 2006, Reverse-time migration using the Poynting vector: *Exploration Geophysics*, 37, 102–107.
- Zhang, Q., and G. A. McMechan, 2011, Direct vector-field method to obtain angle-domain common-image gathers from isotropic acoustic and elastic reverse time migration: *Geophysics*, 76, no. 5, WB135–WB149, doi: 10.1190/geo2010-0314.1.